

μ-X-RAY COMPUTER AXIAL TOMOGRAPHY APPLICATION IN LIFE SCIENCES

I. Tiseanu^a, T. Craciunescu^a, N. B. Mandache^a, O. G. Dului^{a*}

^aInstitute for Lasers, Plasma and Radiation Physics (NILPRP), Măgurele, P.O. Box MG-36, RO -077125, Bucharest, Romania

^bUniversity of Bucharest, Department of Atomic and Nuclear Physics, Măgurele, P.O. Box MG-11, RO - 077125, Bucharest, Romania

X-ray 3D micro-computer tomography has been used to investigate, at a spatial resolution up to 10 μm, the internal architecture of a juvenile exemplar of *Sepia officinalis* L phragmocone. Resulting tomographic images have shown with clarity details of cuttlebone siphuncular zone such as septa and pillars, as well as their insertion zone to hypostracum. At the same time, 3D tomographic images have revealed a local anomaly of the phragmocone consisting of double septa instead of single ones.

(Received March 9, 2005; accepted March 23, 2005)

Keywords: μ-X-ray axial tomography, Phragmocone, Tomograph image

1. Introduction

Since the creation of the first medical Computer Tomograph (CT) in 1973 [1], Computer Axial Tomography (CAT) continuously developed as one of the most versatile techniques for nondestructive control. Developed initially for medical investigations, CAT has been in short applied to various domains such as industry [2,3], archaeology [4], life sciences [5,6] or geosciences [7-9]. Despite a great progress achieved in past decades concerning data acquisition and accuracy in representing investigated objects, the spatial resolution of the best CT was no less than 0.5 mm, totally insufficient to investigate the internal structure at sub-millimeter scale.

This inconvenience has been overcome by construction of micro-focus X-ray tubes [10] with optical focal spot less than 1 μm and development of new reconstruction algorithms specially designed for conic X-rays beams [11] that allowed a direct reconstruction at micron level of the 3D spatial distribution of the Linear Attenuation Coefficient (LAC) of investigated objects. With these new improvements, the micro-CAT (μ-CAT) turned into a noninvasive versatile method currently used not only in scientific research [12-15] but also in the industrial nondestructive control [16-18].

The continuous progress made by the physics of prosthetic materials, and especially of those designed for bone implants has stimulated the use of m-CAT to investigate the microstructure of various kinds of bone tissues [18-20] with remarkable results concerning the osteointegration around metallic implants [19], the role of trabecular architecture [19] or the degree of mineralization [21,22]. As it can be remarked from last references a great volume of work has been done to investigate the inner structure of human and mammalian trabecular bone tissue taking into account two of its main functions, *i.e.* structural support for the mechanical action of soft tissues such as muscles and protective sites for specialized tissues such as the blood-forming system.

* Corresponding author: dului@b.astral.ro

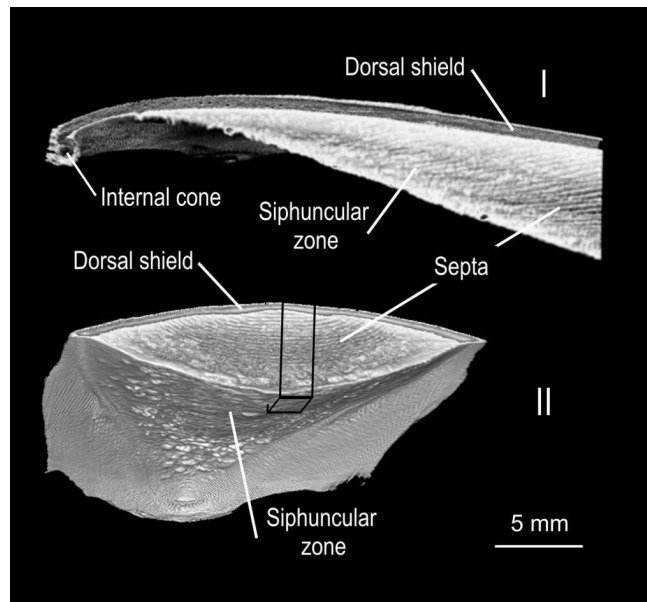


Fig. 1. A longitudinal (I) as well as a transversal (II) section through investigated phragmocone as obtained from the CT reconstructed volume of the specimen. As the reproduced images are positive ones, low densities regions appear in lighter tones of gray than the more dense ones. On the transversal section image the fragment that have been cut to be investigated at a greater magnification is marked by black lines (negative image).

Excepting vertebrates, an inner skeleton that ensures mechanical support can be found only to a very restricted category of Cephalopod invertebrates namely cuttlefish (genus *Sepia*) belonging to Sepiidae family as a part of phylum Mollusca. The inner skeleton of these animals consists of a single calcified shell called phragmocone which plays an important role in cuttlefish biology, assuring both buoyancy and mechanical strength of the body, but, unlike the swim bladders of fish, it keeps its volume almost constant, irrespective of the vertical movements of the animal [23, 24]. To achieve these functions, cuttlebone developed a specific structure, consisting of a succession of parallel chambers and septa that makes it simultaneously light and mechanically resistant, able to withstand hydrostatic pressures up to 45 barr [25].

Until present, the only technique used to investigate the 2D phragmocone inner structure was the confocal optical microscopy [26], but this method could be applied only to relatively thin sections (less than .5 mm), otherwise the object becomes too opaque to be thoroughly analyzed.

By contrary, μ -CAT due to the use of highly penetrating X-ray could investigate objects up to 6 cm thick, allowing to accumulate a significant amount of data about investigated specimen. In addition, by changing the sample position with respect to X-ray tube, it could be obtained different magnifications permitting a better examination.

In this paper we present our experimental results concerning μ -CAT investigation of the internal structure of a *Sepia officinalis* L. phragmocone.

2. Sample

Sepia officinalis L. (cuttlefish) inhabits shallow tropical or temperate coastal waters. Cuttlefishes have rather flattened bodies bordered by a pair of narrow fins, eight arms and two longer tentacles used to capture various kind of living marine animals and a well developed internal, calcified shell, the phragmocone, composed, as in the case of majority marine invertebrates of aragonite, the orthorhombic variety of calcium carbonate.

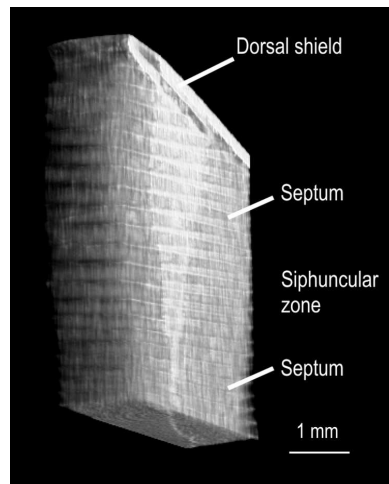


Fig. 2. A 3D tomographic reconstruction of a small fragment extracted from the central region of phragmocone (see Fig. 1). In the vicinity of the dorsal shield (hypostarcum) the septa are smaller as they were formed when the animal was younger.

The investigated specimen, a typical cuttlebone of 92×30 mm with a maximum thickness of 9 mm has been extracted from a specimen bought from a local fish market in Trieste, Italy. By taking into account the number of septa (circa 33) as well as the average sea temperature of 18°C we have estimated the age of investigated specimen at about 100 ± 33 days [27]. As *Sepia officinalis* L. lifespan is about two years, most probably the investigated phragmocone belonged to a juvenile individual.

3. Computer axial microtomography

All tomographic images have been obtained in the μ -CAT laboratory established at NILPRP with European Community support [28]. The μ -Computer Tomograph (μ -CT) was provided with a Phoenix X-Ray Microfocus open X-ray tube type 160 kV (maximum high voltage of 160 kVp at 20 W maximum power), while the transmitted X-rays have been detected by means of a Siemens Medical Solutions SIRECON 17-2 HDR-M X-ray image intensifier, coupled with a CCD-Compact-Camera. A 10 bits analog frame grabber National Instruments IMAQ PCI-1409 was used for images acquisition. Depending on the reproduction scale, the reduction in distortion for the total imaging chain (image intensifier, lenses and CCD) varied between 3% and 7%. The detector was placed on a manually adjustable table with vertical and transversal positioning. Alternatively the transversal position of the detector could be adjusted using a computer controlled micrometric motorized stage. The investigated sample was placed on a micrometric manipulator, where two Sigma-Koki, (Japan) motorized stages were combined to assure a maximum degree of freedom in positioning. In order to realize an x - z - θ assembly the positioning system is provided with two translations and one rotation axes.

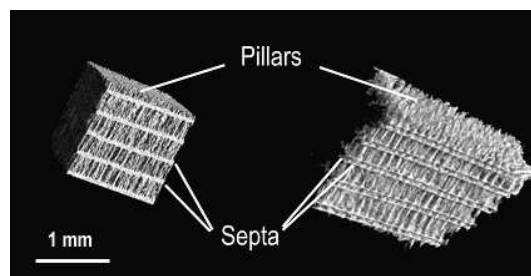


Fig. 3. 3D tomographic reconstructions of two small pieces detached from the lower part of the segment reproduced in Fig. 2. On both fragments septa as well as pillars can be very well observed. Looking at the superior part of both segments, pillars seem to be erratically distributed (negative image).

The image acquisition, 3D reconstruction and reconstructed volume visualisation have been carried out by two networked Dual CPU (2 GHz, 2GB) workstations. Both image acquisition and motorized stage control programs were developed on the base of the National Instruments LabView Virtual Instruments library. Usually, an object has been scanned for 360 to 720 projections. The 3-D tomographic reconstructions were obtained by a proprietary highly optimized computer code based on a modified Feldkamp algorithm [11]. In this way, the 3D reconstruction time varied between 2 minutes for a $256 \times 256 \times 256$ lines volume and 20 minutes for a $1024 \times 1024 \times 512$ lines volume for a final optical resolution better than $10 \mu\text{m}$ and a LAC accuracy of about 1 %.

4. Results and discussion

To get as much as possible information concerning the considered cuttlebone, we have investigated it at different magnifications, by gradually decreasing the distance between sample and X-ray tube focal spot at a constant focal spot – detector distance. In this way, the smaller the sample to focal spot distance, the greater magnification was.

In Fig. 1 two low magnifications ($\times 3$) 3D reconstructions of the posterior half of the cuttlebone are reproduced. Both images resulted from the same set of experimental data containing numerical values of the linear attenuation coefficient of the cuttlebone material. Since we have investigated a desiccated phragmocone, its tomographic images are very easy to interpret as at present time it consists mainly of calcium carbonate and voids. As reproduced images are positive ones, the higher the density the darker gray shades appears on tomographic images. For that reason dorsal shield or hypostracum as well as the septa that delimitate phragmocone chambers appears in darker tones of gray. On these images different details of structure such as dorsal shield, growth septa or the internal cone existent at the posterior extremity of cuttlebone are well illustrated. A more careful inspection has showed on both images a gradual increasing of the cuttlebone density towards its center, most probably connected with an improved mechanical strength. Another details of structure well represented on the second image are the parallel ripples of the posterior lateral wings of the dorsal shield symmetrically disposed along the siphuncular zone.

More details concerning the local structure, we have obtained by extracting from the central part of cuttlebone a prismatic fragment of about $2.2 \times 2.2 \times 9$ mm that has been investigated at a significant higher magnification ($\times 25$). The resulted tomographic image, reproduced in Fig. 3, shows with clarity the dorsal shield, septa as well as the pillars that connect them. At a carefully examination, on the right hand side of the phragmocone fragment, it can be noticed an anomaly of septa consisting of a duplication of them, most probably a healed fracture. The extent of this anomaly can be very easy observed as it appears in darker hues, a characteristic of zones with increased density.

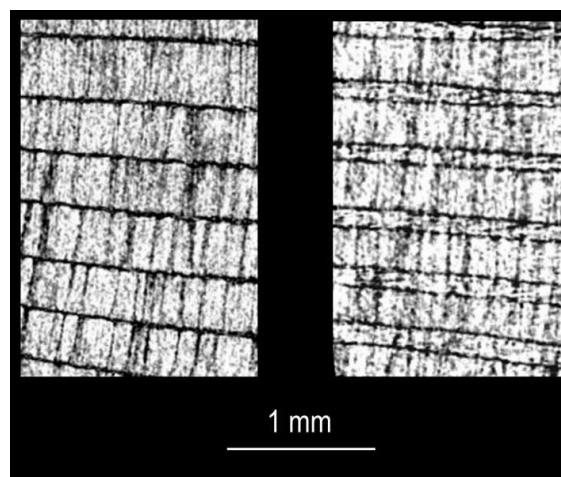


Fig. 4. Two thin sections, parallel to pillars, through the fragments reproduced in Fig. 3.

Further, we have detached two small rectangular pieces of about $1.5 \times 1.5 \times 1.4$ mm from normal and fractured bone fragment as well as a segment of about 1.5 mm of hypostracum for a detailed examination at an even higher magnification (x 38). At this magnification we have obtained a set of tomographic images (Fig. 3 and 4) that reproduce with a spatial resolution of approximately $7 \mu\text{m}$ the microscopic structures of the phragmocone. On both figures similar structure consisting of septa connected by a set of pillars can be distinguished. The difference between two images consists of that on the left, undamaged bone the septa are equally spaced, at an average distance of $360 \pm 51 \mu\text{m}$, coincident within the experimental uncertainties with those reported in [26] for a similar taxon, while in the damaged area, we have measured two different distances, one of $340 \pm 47 \mu\text{m}$ between septa that delimitate a chamber and and the $75 \pm 8 \mu\text{m}$ between double septa. At the same time, by using adequate software (VGStudioMaxTM from Volume Graphics) we have obtained two virtual thin sections, perpendicular to the septa, for both sub-fragments (Fig. 4).

The last ones images, show, that irrespective of the septa structure, all pillars that connect septa are parallel, suggesting that the pillars growth mechanisms was the same on both damaged and undamaged sections. On this image, pillars as well as septa thickness are almost the same and equal to about $15 \mu\text{m}$. The image of the undamaged area are comparable to those presented in [26], with the only difference that in the case of ref. [26], images have been obtained by means of confocal microscopy. Somewhat different appears the image of presumably damaged bone where we have noticed duplicated septa, unevenly connected by pillars. It is worth to mention that even on these images, the septa as well as pillar thickness are the same as in the undamaged area. Although it is difficult to make any assumption concerning the origin of this abnormally, the observed structure represents interesting details of the phragmocone structure, which once more confirms the great possibilities offered by μ -CAT in investigation the invertebrate skeleton.

In spite of the fact that the investigated sections have shown no spatial regularity in pillars disposition, the inner face of hypostracum preserves not only the insertion zones of septa, but also present some undulated formations connecting these zones that can be regarded as pillar insertions (Fig. 5).

In this way, by gradually increasing the magnification, we have been able to obtain a full scale phragmocone representation, beginning with the entire specimen and ending with the smallest details. It must be pointed out that, by respect to traditional confocal microscopy [26], μ -CAT can generate true 3D images as well as pictures of any section through an object, this peculiarity representing in our opinion a significant improvement.

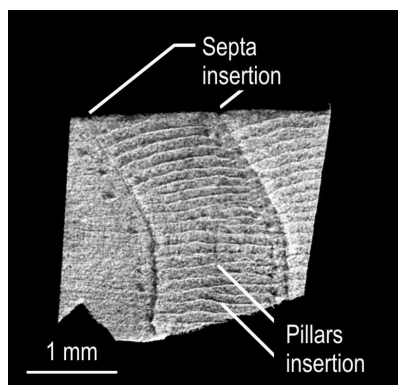


Fig. 5. A 3D tomographic reconstructions of the siphuncular face of a fragment of the dorsal shield. Both septa and pillars insertions can be observed. By contrary to siphuncular zone where pillars appear to be disposed randomly, on this face the pillars form almost parallel rows.

4. Concluding remarks

X-ray 3D micro-computer tomography has been used to investigate, at a spatial resolution up to $10 \mu\text{m}$, the internal architecture of a juvenile exemplar of *Sepia officinalis* L phragmocone.

The phragmocone is a notable organ that ensures both buoyancy and mechanical strength of a soft-bodied animal like cuttlefish. To achieve these contradictory functions, cuttlebone has developed a particularly intricate structure, best revealed by means of nondestructive 3D micro-computer tomography. Resulting tomographic images have shown with clarity details of cuttlebone siphuncular zone such as septa and pillars, as well as their insertion zone to hypostracum. At the same time, 3D tomographic images have shown a local anomaly of the phragmocone consisting of double septa instead of single ones, most probably a healed fracture.

These results have proved the vast field of applicability of nondestructive 3D micro-computer axial tomography in investigating complex anatomic structures.

References

- [1] G. N. Hounsfield, British Patent No. 1283915, British Patent Office, London, (1972).
- [2] L. A. G. Aylmore, *Advan. Agron.* **49**, 1 (1993).
- [3] O. G. Dului, F. Preoteasa, C. T. Rizescu, G. G. Georgescu. *J. Trace Microprobe Tech.* **21**, 493 (2003).
- [4] A. Taylor. *Egyptian Archaeology* **4**, 145 (1994).
- [5] P. B. Fransham, J. Jelen. *J. Canad. Petrol. Tech.* **26**, 42 (1987).
- [6] M. Iovea, A. Vamvakoussis, G. Mateiasi, V. Georgiou, G. Samoilis, M. Neagu, *Insight* **43**, 362 (2001).
- [7] P. Jacobs, E. Sevens, M. Kunnen. *Sci. Tot. Envir.* **167**, 161 (1995).
- [8] W. D. Carlson, T. Rowe, R. A. Ketcham, M. W. Colbert, (eds. F. Mees, R. Swennen, M. Van Geet, and P. Jacobs). Geological Society, London Special publication no. 215, 7 (2003).
- [9] O. G. Dului. *Earth Sci. Rev.* **48**, 265 (1999).
- [10] M. Wevers, P. de Meester (2000)
<http://www.ndt.net/article/wcndt00/papers/idn399/idn399.htm>.
- [11] L. A. Feldkamp, L. C. Davis, J. W. Kress. *J. Opt. Soc. Amer.* **1**, 612 (1984).
- [12] B. P. Flannery, H. W. Deckman, W. G. Roberge, K. L. D'Amico. *Science*, **237**, 1439 (1987).
- [13] V. Cnudde, P. Jacobs. *Environ. Geology* **46**, 477 (2004).
- [14] E. N. Landis, A. L. Petrell, S. Lu, E. N. Nagy. *Concrete. Sci. Engng.* **2**, 162 (2000).
- [15] C. Coléou, B. Lesaffre, J. B. Brzoska, W. Ludwig, E. Boller. *Annals of Glaciology* **32**, 75 (2001).
- [16] K. Vandersteen, B. Busselen, K. Van den Abeele, J. Carmeliet, (eds. F. Mees, R. Swennen, M. Van Geet, and P. Jacobs). Geological Society, London Special publication no. 215, 61 (2003).
- [17] A.-H. Benouali, L. Froyen, M. Wevers. In *X-ray Tomography in Materials Science*, (eds. J. Baruchel, J.-Y. Buffière, E. Maire, P. Merle, G. Peix.), Hermes Science Publications, Paris, 139 (2000).
- [18] S. Nuzzo, M. H. Lafage-Proust, E. Martin-Badosa, G. Boivin, T. Thomas, C. Alexandre, F. Peyrin. *J. Bone. Miner. Res.* **17**, 1372 (2002).
- [19] P. Ruegsegger, B. Koller, R. Müller. *Calcif. Tissue Int.* **58**, 24 (1996).
- [20] M. J. Jaasmaa, H. H. Bayraktara, G. L. Nieburb, T. M. Keavenya. *J. Biomechan.* **35**, 237 (2002).
- [21] W. Pistoia, B. Van Rietbergen, E.-M. Lochmüller, C. A. Lill, F. Eckstein, P. Ruegsegger, *Bone*, **30**, 842 (2002).
- [22] S. Nuzzo, F. Peyrin, P. Cloetens, J. Baruchel, G. Boivin. *Med. Phys.* **29**, 2672 (2002).
- [23] E. J. Denton, J. B. Gilpin-Brown. *Mar. Biol. Assoc. UK*, **41**, 319 (1961).
- [24] E. J. Denton. *Proc. R. Soc. Lond. B.* **185**, 273 (1974).
- [25] W. Adam, W. Rees. *The John Murray Expedition, Scientific Reports* **11**, 165 (1966).
- [26] K. M. Sherrard. *Biol. Bull.* **198**, 404 (2000).
- [27] V. Bettencourt, A. Guerrero. *Mar. Biol.* **139**, 327 (2001).
- [28] Tiseanu, C. Sauerwein, M. Simon, M. Misawa, Annual Meeting of Nuclear Technology, May 2002, Stuttgart, Germany.
- [29] Tiseanu, EFDA Fusion Newsletter, **6**, 4, (2003).
(http://www.efda.org/downloading/newslett/nl_december_03.pdf).